

MIT LIBRARIES



3 9080 02754 4706

V393  
.R46



DEPARTMENT OF THE NAVY

HYDROMECHANICS

MEASUREMENTS OF THE FLUCTUATING STATIC AND TOTAL-HEAD  
PRESSURES IN A TURBULENT WAKE

○

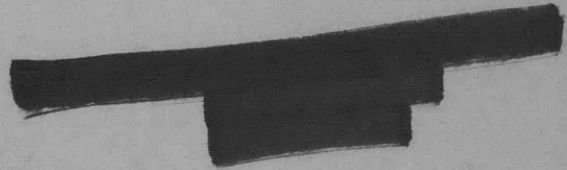
by

AERODYNAMICS

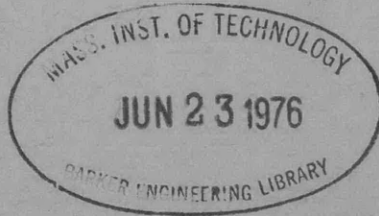
M. Strasberg

○

STRUCTURAL  
MECHANICS



○

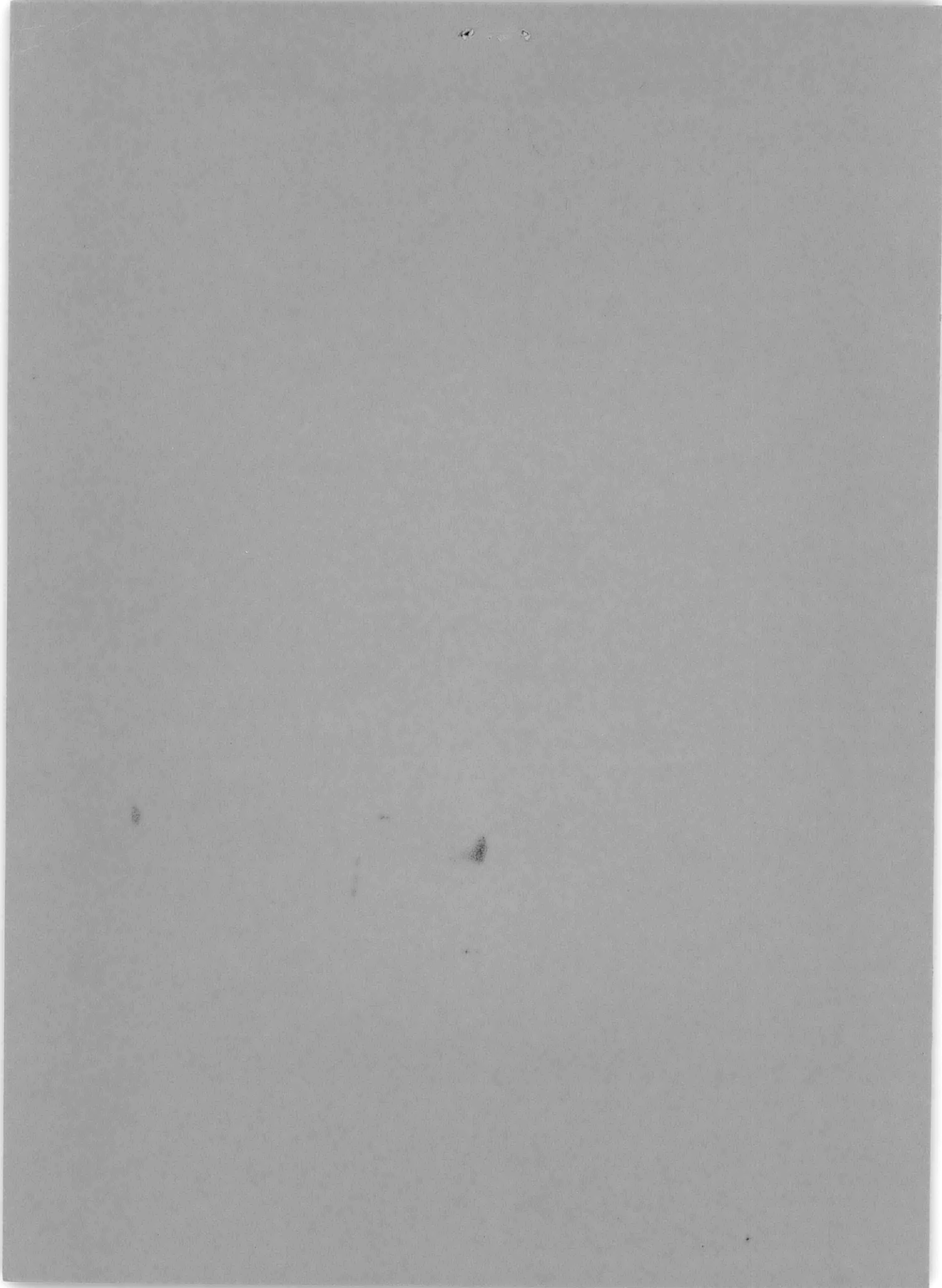


APPLIED  
MATHEMATICS

RESEARCH AND DEVELOPMENT REPORT

December 1963

Report 1779



MEASUREMENTS OF THE FLUCTUATING STATIC AND TOTAL-HEAD  
PRESSURES IN A TURBULENT WAKE

by

M. Strasberg

This report is based on a paper presented at a Symposium on the "Mechanism of Noise Generation in Turbulent Flow," held at the Training Center for Experimental Aerodynamics, Brussels, Belgium, 1-5 April, 1963, under the sponsorship of the AGARD Panel on Fluid Dynamics.

December 1963

Report 1779

## TABLE OF CONTENTS

	Page
ABSTRACT .....	1
1. INTRODUCTION .....	1
2. APPARATUS .....	2
2.1 Wind Tunnel .....	2
2.2 Pressure Probes .....	3
2.3 Electronic Instrumentation .....	5
3. RESULTS .....	7
3.1 Fluctuating Static Pressure .....	7
3.2 Correlation of Static Pressure and Velocity .....	8
3.3 Fluctuating Total Head .....	9
3.4 Correlation of Total Head and Velocity .....	10
4. DISCUSSION .....	10
4.1 Probe Errors .....	10
4.2 Comparison with Theory .....	13
4.3 The Spectra .....	14
4.4 Comparison with Other Data .....	15
4.5 Fluctuating Total Head .....	15
5. CONCLUSIONS .....	17
6. REFERENCES .....	24

## LIST OF FIGURES

	Page
Figure 1 - Schematic of the Total-Head Probe Attached to the Capacitance Microphone Cartridge, and the Static-Pressure Probe .....	18
Figure 2 - Annular Ring Slit in the Static-Pressure Tube .....	18
Figure 3 - Response of Total-Head Probe Tube and Microphone .....	18
Figure 4 - Block Diagram of Electronic Instrumentation .....	19
Figure 5 - Typical Spectra, Plotted by Automatic Recording Frequency Analyzer, for Two Frequency Ranges .....	19
Figure 6 - Fluctuating Static Pressure, as a Function of Transverse Coordinate $y$ , at Various Downstream Locations .....	20
Figure 7 - Nondimensional and Normalized Spectral Density of Fluctuating Static Pressure and Velocity at $x/D = 24$ , $y/D = 1/2$ .....	20
Figure 8 - Measured Root-Mean-Square Value of Total Fluctuating Static Pressure and Velocity as a Function of Reynolds Number at $x/D = 24$ , $y/D = 1/2$ .....	21
Figure 9 - Simultaneous Oscillograms of Fluctuating Velocity and Static Pressure .....	21
Figure 10 - Comparison of the Spectral Densities Determined with a Total-Head Probe and a Hot Wire .....	22
Figure 11 - Transverse Correlation ( $\overline{u_1 p_2}$ ) of Signals from a Total-Head Probe and a Hot Wire Compared with Correlation ( $\overline{u_1 u_2}$ ) of Signals from Two Wires .....	23

## NOTATION

D	Diameter of the cylinder
F(S)	Normalized dimensionless spectral density; $\int_0^{\infty} F(S)dS = 1$
L	A length in the correlation function $e^{- x' /L}$
n	Frequency in cycles per unit time
p <sub>m</sub>	Instantaneous measured pressure (in the probe tube)
p <sub>s</sub>	Instantaneous true static pressure
p <sub>t</sub>	Instantaneous total-head pressure
S	Strouhal number; $S = nD/U_0$
U	Local mean velocity in the x-direction
U <sub>0</sub>	Free-stream velocity
u	Instantaneous fluctuating velocity component in the x-direction
$\tilde{u}$	Root-mean-square value of u
v <sub>t</sub>	Instantaneous transverse velocity, normal to the probe tube
x	Coordinate in downstream direction
x'	Separation of two points in the x-direction
y	Coordinate perpendicular to both x and the axis of the cylinder
—	Signifies a time average.
~	Signifies an rms (root-mean-square) value.

## ABSTRACT

The use of probe tubes for measuring the fluctuating "static" and stagnation-point pressures in subsonic turbulent wakes is discussed and estimates are made of the magnitude of several sources of error. It is shown that the mere presence of a probe tube in a turbulent flow causes the measured mean-square value of the fluctuating static pressure to exceed the true value by about  $\frac{1}{4}(\overline{\rho v_t^2})^2$ , where  $v_t$  is the fluctuating velocity component normal to the tube. Although this error is just about equal to the magnitude of the fluctuations expected in isotropic turbulence, the fluctuations in shear flows can exceed the error by enough to be measurable. The results of measurements of fluctuating pressure made in the wake behind a cylinder are presented. Data are given on the rms values and the spectra of the fluctuating static and total-head pressures, and on the cross correlations of these pressures with the fluctuating velocity.

### 1. INTRODUCTION

Although measurements of the fluctuating pressure at a wall bounding a turbulent flow have now become almost commonplace, measurements made away from the wall, or within an unbounded region, are still rare. Probably the main reason for this deficiency is the lack of completely satisfactory instrumentation for measuring the fluctuating "static" pressure within a fluid. The obvious way to perform such a measurement is to use a static pressure probe tube and to replace the conventional manometer with an electrical transducer which responds to fluctuating pressure. The presence of the probe tube will disturb the flow, however, and the question arises as to how much error will result. It is well known that the impact of the fluctuating cross velocities on the wall of a probe tube causes the steady<sup>1</sup> indication of a static pressure probe to exceed the true static pressure; the fluctuating part of the static pressure may certainly be even more affected, since the fluctuations in pressure are entirely dependent on the velocity fluctuations.

---

<sup>1</sup>References are listed on page 24.

Accordingly, when R. Cooper and the present writer first described our measurements of fluctuating static pressure made with a probe tube in the wake behind a cylinder,<sup>2</sup> we expressed some doubt about the validity of our results. Since then, we have been able to perform additional measurements with improved probe tubes. These measurements, together with some elementary analytical considerations, have satisfied us that the measured values of the fluctuating static pressure are, indeed, approximately correct. Because the results reported previously were given only limited distribution, this present opportunity will be used to describe all our measurements of fluctuating pressure, the old as well as the new, in greater detail.

In addition to the static-pressure fluctuations, the fluctuations in total head, or stagnation-point pressure, were measured at the nose of an impact tube. The total-head fluctuations have some practical interest because of the possibility that they can be used as a measure of the longitudinal component of the turbulent velocity.<sup>3,4</sup> Although the use of hot wires for turbulence measurements in air is well developed, so much trouble is experienced when hot wires are used in water that other devices warrant consideration for this application. The measurements reported herein were made in air, and included simultaneous measurements with a hot wire so that the amplitudes and spectra indicated by the two instruments could be compared. The cross correlation of the signals from the total-head probe and the hot wire was also measured, thus providing a sensitive basis for comparing the outputs of the two instruments.

Several other attempts have been made to measure the static-pressure fluctuations in a turbulent flow. Rouse<sup>5</sup> used a probe tube with several holes set in the hemispherical nose at angles chosen to reduce the error due to the fluctuating cross velocities. Kobashi<sup>6</sup> has reported measurements behind a cylinder using a probe tube with side holes. Measurements of a fluctuating total head have been discussed in several papers.<sup>3,4,7,15</sup>

## 2. APPARATUS

### 2.1 WIND TUNNEL

The measurements were performed in a low-turbulence, open-return



subsonic wind tunnel with a test section 2 ft wide and 4 ft high. The cylinder spanned the entire test section vertically. Most of the measurements used a 1-in. cylinder, but some data were obtained at higher Reynolds numbers with a 4-in. cylinder. Both cylinders were standard brass tube stock without any special surface finish.

The floor of the test section had a motordriven carriage supporting the pressure probe and the hot wire so that they could traverse the wake automatically and continuously.

## 2.2 PRESSURE PROBES

The pressure probes consist of short, straight tubes terminated by a small microphone. The final designs of the total-head and static-pressure probes are shown schematically in Figure 1. The external diameter of the tubes is  $3/32$ -in. and the length is 2 to  $2\ 1/2$  in. The total-head tube is open at the forward end to its full external diameter. The static-pressure tube has an annular ring slit  $1/2$  in. behind its hemispherical nose; the pressure at this slit communicates to the microphone through grooves inside the tube, as shown in the detail drawing, Figure 2.

Both tubes are used with the same microphone, which is a commercial unit, Type 21-BR-180, manufactured by the Altec Lansing Company. The microphone is of the variable capacitance type, comprising a thin diaphragm held about 1 mil in front of a rigid back plate to form an air-gap capacitor. A change in pressure on the diaphragm changes its separation from the back plate, and the resulting change in capacitance is converted into an electrical signal. The microphone is in the form of a short cylindrical cartridge about  $3/4$  in. in diameter. The probe tube screws onto the front of the cartridge, and the back of the cartridge screws into a tubular housing of a preamplifier of the same diameter and about 6 in. long.

The ring slit on the static-pressure tube represents the final version of several designs. Other tubes were used with one, two, and four side holes instead of the ring slit, and one tube was twice the diameter of the present tube. As will be discussed later, the data obtained with all these probes were in substantial agreement.

A capacitance sensing element was chosen in preference to a piezoelectric transducer for two reasons: (1) it is much less liable to

generate spurious signals when subjected to vibration and (2) it generates a much larger voltage; its sensitivity of about 0.5 millivolts per dyne/cm<sup>2</sup> is perhaps 1000 times greater than that of conventional piezoelectrics of comparable size.

The dimensions of the probe tube represent a compromise between opposing requirements. Aerodynamic considerations require that the tube have the smallest possible diameter and the greatest permissible length, just as with conventional tubes for measuring steady pressures. However, just the opposite requirements must be met in order that the probe have uniform sensitivity to pressure fluctuations over the widest possible frequency range.

To achieve uniform sensitivity, the pressure communicated to the microphone diaphragm should equal that at the tube opening at all frequencies. Two effects, both associated with the compressibility of the air, militate against this, however. First, the pressure fluctuations propagate down the tube as an acoustic wave. If the tube is long enough, standing waves are set up, causing resonant increases in sensitivity. In a tube 2 in. long, the first standing-wave resonance occurs at only about 1500 cycles/sec. Second, the mass of air in the tube, together with the compressible air in the cavity between the microphone diaphragm and the tube, forms a Helmholtz resonator which has a resonant response and reduced sensitivity at frequencies above resonance. Detailed analyses of these effects have been published.<sup>8,9</sup>

Since uniform response occurs only for frequencies below resonance, it is desirable to push the resonant frequency as high as possible. The resonant frequency  $f_r$  can be estimated by solving for  $R$  in the equation

$$R \tan R = \pi a^2 T / V, \quad [1]$$

where  $R = 2 \pi f_r T / c$ , with  $T$  the length and  $a$  the radius of the tube,  $V$  the cavity volume, and  $c$  the velocity of sound in the gas. It is apparent that the resonant frequency is highest for short, large-bore tubes. A reduction in cavity volume also raises the resonant frequency; for this reason, the rear end of the probe is designed to fill up most of the cavity in front of the diaphragm; see Figure 1.

The sharp rise in response at resonance can be eliminated by providing viscous dissipation inside the tube. This is done with a small plug of absorbent cotton. The correct amount of cotton was determined by trial and error as follows: The microphone, without the probe tube, was placed in the tunnel test section and an acoustic noise source was placed at the tunnel intake. The output of the microphone in response to the noise was then measured at various frequencies in the range of interest. The probe tube was then attached to the microphone, with the tube opening at the same location as the bare microphone, and the output was measured again. Any difference in output was due to the tube. With no cotton in the tube, a characteristic resonant response was observed in the frequency range 700 to 1000 cycles/sec, typically amounting to an increase in sensitivity by a factor of 3 to 5. A tiny plug of cotton was then inserted into the diaphragm end of the tube and the new response determined as above. This procedure was repeated with various amounts of cotton until the best, or "flattest," response was obtained.

The response of the total-head probe actually used is shown in Figure 3. The static-pressure probe has about the same response.

The microphone is sensitive enough for its absolute sensitivity to be determined by conventional acoustical techniques involving small-amplitude sinusoidal pressure fluctuations. The calibration is performed by comparing the output of the microphone, in response to sinusoidal pressure at various frequencies, with the output of another microphone of the same type used as a reference standard. This comparison is made by attaching the two microphones in sequence to an acoustic coupler, General Radio Type 1552-B, this being a small rigid-walled cylindrical cavity with a miniature loud speaker on one end. The sensitivity of the microphone used as a standard was determined at the National Bureau of Standards using an absolute calibration procedure known as a "reciprocity calibration."<sup>10</sup> The sensitivity determined in this way is believed to be accurate to  $\pm 5$  per cent.

### 2.3 ELECTRONIC INSTRUMENTATION

The instrumentation for handling the electrical signals from the wire and the probe is indicated in the block diagram, Figure 4. The

frequency spectrum of either signal can be obtained with an automatic recording frequency analyzer Type 3A-4A, manufactured by the Technical Products Company. This equipment automatically plots the spectrum on a chart about 10 in. long. The effective bandwidth chosen for the spectrum filter was 30 cycles/sec, and about 10 min was used to sweep through the frequency range up to 1500 cycles/sec.

The waveform of wire and probe signals can be observed simultaneously on a dual-beam oscilloscope. The correlation of the two signals was determined by the sum-and-difference method, the signals being combined in a bridge circuit.

The hot wire was operated in a constant-temperature d-c feedback circuit developed at the Iowa Institute of Hydraulic Research. Only the longitudinal component of velocity was measured.

The signal amplitudes were determined with the full-wave linear rectifier built into the recording analyzer. The use of such a simple rectifier, instead of the more complicated squaring and averaging devices usually employed, may be worth discussion. The magnitudes of interest are, of course, the mean-square or rms values. These values can be deduced from the output of a linear rectifier if the instantaneous amplitude distribution of the signal is known. For a signal with Gaussian probability density, the rms value is larger than the linear rectified value by the ratio 1.25; whereas for a sinusoidal signal the ratio is only 1.11. Accordingly, if Gaussian and sinusoidal signals have the same linear-rectified value, the Gaussian signal will have an rms value larger by a factor  $(1.25/1.11)$ , or 1.13. Since the electrical calibrations of the instruments were performed with sinusoids and the turbulence signals are assumed to be Gaussian, the rms values of the turbulence signals were obtained by multiplying the readings by 1.13. It is believed that any deviation from Gaussian that might exist in the actual turbulence signal would result in an error much smaller than the overall precision of the measurements.\*

---

\*The ratio of 1.25 assumed here is, in fact, the value actually observed by Roshko<sup>11</sup> in his measurements of the turbulent longitudinal velocity behind a cylinder.

### 3. RESULTS

#### 3.1 FLUCTUATING STATIC PRESSURE

The frequency spectrum of the fluctuating static pressure consists of a continuous spectrum associated with random fluctuations, plus superimposed discrete frequency components associated with vortex shedding. The significance of these two types of contribution to the spectrum is discussed in greater detail by Roshko<sup>11</sup> in connection with velocity fluctuations. The two contributions show up distinctly in the photograph, Figure 5, of typical frequency analyses plotted by the automatic recording analyzer for two frequency ranges. The peak near 70 cycles/sec is associated with a discrete frequency component at the frequency of vortex shedding, whereas the remainder of the spectrum is continuous. The broadening of the peak is a result of the finite bandwidth of the filters in the frequency analyzer. Analyses made with two bandwidths are superposed on the upper analysis. For a discrete frequency, the amplitude transmitted by a filter is independent of the filter bandwidth; accordingly, the fact that both bandwidths indicate the same amplitude is proof that the component is indeed a single frequency, or at least is concentrated in a band that is smaller than the narrower filter. On the other hand, the continuous spectrum, apparent in the plot at the frequencies above 90 cycles/sec, is higher in the wider band by an amount just equal to the ratio of the two bandwidths.\*

Traverses across the wake behind the cylinder are shown in Figure 6, where the variation in the amplitude of the static pressure fluctuations is plotted as a function of the transverse coordinate  $y$  for several distances  $x$  downstream of the cylinder. The left-hand set of traverses gives the mean-square pressure  $p_1^2$  at the frequency of vortex shedding (corresponding to a Strouhal number  $S = nD/U_0$  of about 0.21), whereas the right-hand set

---

\*Note that the amplitude scale is logarithmic, each fine division corresponding to .1 db, or a factor of  $10^{0.1}$  in mean square, so that a bandwidth ratio of 4 corresponds to 6 db.

shows the dimensionless spectral density of the continuous spectrum at a frequency some five times higher. Note that the ordinate scale is logarithmic; thus the mean-square pressure at the shedding frequency falls by a factor of about 1000 from  $x/D = 1.5$  to  $x/D = 24$ . In fact, 24 diameters downstream the shedding frequency can barely be discerned from the continuous spectrum and at larger distances it is not discernible at all. This effect was also observed by Roshko for the velocity fluctuations.

Spectra of both the pressure and velocity fluctuations at  $x/D = 24$ ,  $y/D = 1/2$  are shown in Figure 7. The ordinate scale is the nondimensional spectral density  $F(S)$ , normalized on Strouhal Number so that  $\int_0^{\infty} F(S) dS = 1$ . Both coordinates are plotted logarithmically; note that the velocity ordinate has been shifted by a factor of 100 to separate the velocity and pressure points. The plotted points cover a range of Reynolds number from  $7 \times 10^3$  to  $1.2 \times 10^5$ ; the relatively small scatter indicates that Reynolds number effects are small in this range.

The total rms static-pressure fluctuation is plotted as a function of Reynolds number as the lower curve of Figure 8, nondimensionalized by dividing by the dynamic pressure  $1/2 \rho U_0^2$ . Values are plotted for measurements obtained with both the 3/32- and the 3/16-in.-diameter probes, the small probes having either 4 side holes or the ring slit shown in Figure 2, and the larger having only 1 hole. No significant differences in the rms values were observed with these probes; although not shown, no significant differences were observed in the spectra obtained with the various probes either. The plotted points do not show any discernible trend with varying Reynolds number. The average line drawn through the points indicates a measured value of the fluctuating static-pressure coefficient  $(\tilde{p}/\frac{1}{2}\rho U_0^2)$  equal to 0.035. This value holds, of course, only for  $x/D = 24$ ,  $y/D = 1/2$ . The rms velocity fluctuation  $\tilde{u}$  measured with the hot wire is also indicated on Figure 8; the values agree quite well with Fage's value<sup>1</sup> obtained by visual observations at about the same downstream position.

### 3.2 CORRELATION OF STATIC PRESSURE AND VELOCITY

The correlation between the fluctuating longitudinal velocity and static pressure was determined with the hot wire placed as close to the probe hole as possible, actually 1/8 in. from the probe axis in the

y-direction. At downstream positions close to the cylinder, the correlation was measurable; e.g., the coefficient of correlation was about 0.3 at  $x/D = 3$ . At greater distances, e.g., at  $x/D = 24$ , no measurable correlation could be observed with the sum-and-difference equipment, indicating a correlation coefficient less than 0.01.

The nature of the correlation is indicated by the simultaneous oscillograms of the two signals shown in Figure 9, where the upper trace of each pair is velocity and the lower is static pressure. The vortex shedding frequency is predominant in both signals at  $x/D = 3$ . The lower left pair of traces is for the same location, but both signals have been passed through band filters centered at the shedding frequency to eliminate the random turbulence fluctuations. It is of interest that both velocity and static-pressure signals show intermittent fluctuations in the amplitude of the shedding frequency component, but the fluctuations are not related in time. The pair of traces on the lower right shows the random, uncorrelated fluctuations characteristic of the turbulent wake at  $x/D = 24$ .

### 3.3 FLUCTUATING TOTAL HEAD

Only a limited amount of data were obtained with the total-head tube. To a first approximation, the instantaneous fluctuating total-head pressure  $p_t$  should be proportional to the instantaneous fluctuating longitudinal velocity  $u$ , viz.,

$$p_t / \rho U_o^2 = (u / U_o); \quad [2]$$

see, e.g., References 3 and 15.

The purpose of these measurements was to compare the magnitude of the fluctuating velocity, calculated by applying the above expression to the measured pressure, with the value indicated by a hot wire. A comparison of the total rms signals from the two instruments is given in Table 1, for three downstream locations. The agreement is good except at the closest position.

TABLE 1  
Comparison of Hot Wire and Total-Head Signals

Location		Hot Wire	Total Head
x/D	y/D	$\tilde{u}/U_o$	$\tilde{P}_t/\rho U_o^2$
4	1/2	0.22	0.20
12	0	0.14	0.14
24	0	0.10	0.10

A comparison of the dimensionless spectra of the two signals is shown in Figure 10 for location  $x/D = 24$ ,  $y = 0$ . The two spectra are in good agreement.

### 3.4 CORRELATION OF TOTAL HEAD AND VELOCITY

The transverse correlation of fluctuating longitudinal velocity with total head is shown in Figure 11 as a function of the transverse (y-direction) separation of hot wire and pressure probe. For comparison, the transverse correlation indicated by two hot wires is also plotted. It is apparent that the correlation between total head and velocity is substantially lower than the true velocity correlation.

## 4. DISCUSSION

The general characteristics of the fluctuating static pressure behind a cylinder observed in these measurements are already familiar, being essentially the same as those of the velocity fluctuations described by Roshko.<sup>11</sup> Close to the cylinder, the fluctuations have a strong component at the frequency of vortex shedding, but this component decays more rapidly than does the continuous spectrum of the random turbulent fluctuations and is submerged in the continuous spectrum at distances more than 24 cylinder diameters downstream.

### 4.1 PROBE ERRORS

The first question to consider is the one raised in the introduction: Does the static-pressure probe indicate the true static pressure? Intuitively, it would seem that a spurious increment of fluctuating pressure



will result from the impact of the fluctuating cross velocities on the probe tube. These fluctuations might be of opposite sense on opposite sides of the tube, however, so some cancellation of the spurious pressure might occur inside a tube having an axisymmetric opening such as the ring slit.

One might assume, naively, that the magnitude of the spurious pressure could be estimated by measuring the change in steady pressure when the tube is set at a steady angle of yaw relative to the mean flow. However, the effect of steady yaw is entirely different from that of turbulent flow, as has been pointed out by Goldstein,<sup>1,2</sup> because steady yaw results a "deadwater" region on one side of the tube. In fact, the steady increment of pressure is usually negative for steady yaw, whereas it is positive for turbulence.<sup>1</sup>

An elementary analysis of the effect of the cross velocities can be made by expressing the pressure perturbation caused by them as a series of terms involving successively higher powers of the velocities. For an axisymmetric tube pointing in the direction of the steady flow  $U_0$ , it is convenient to decompose the instantaneous vector velocity into an axial component ( $U_0 + u$ ) and a transverse component  $v_t$  normal to the tube. In terms of these components, the differences between the instantaneous values of the measured pressure  $p_m$  inside the tube and the true static pressure  $p_s$  can be expressed as a power series

$$\frac{p_m - p_s}{\rho U_0^2} = A + B \frac{u}{U_0} + C \left( \frac{u}{U_0} \right)^2 + D \frac{v_t}{U_0} + E \left( \frac{v_t}{U_0} \right)^2 + F \frac{uv_t}{U_0^2} + \dots \quad [3]$$

where A, B, C, etc., are coefficients to be evaluated.

It is immediately apparent that A is simply the steady pressure coefficient of the opening. Secondly, if one considers the perturbation due to an entirely axial flow of varying speed, it becomes apparent that  $B = 2A = 2C$ . If the side opening is far enough from the nose and from the expanded aft end of the tube, the steady pressure coefficient A will be

very small so that B and C will also be very small.\* Third, the coefficients D and F are zero because of the axial symmetry of the probe tube, i.e., because the tube cannot distinguish a positive value of transverse velocity (going away from the tube on one side) from a negative one (going toward the tube on the same side). This leaves only E to be determined.

If time averages are taken of the only terms remaining in Equation [3], the equation  $\bar{p}_m - \bar{p}_s = E \rho \overline{v_t^2}$  results. The coefficient E can thus be determined from the steady increment of static pressure in a turbulent flow. This increment has already been determined by Fage;<sup>1</sup> with his value, Equation [3] becomes

$$p_m - p_s = 0.25 \rho v_t^2 \quad [4]$$

This equation differs from Fage's in that it applies to instantaneous values. The difference between the fluctuating portions  $p_m'$  and  $p_s'$  of the two pressures can be obtained by subtracting the time average  $\bar{p}_m$  and  $\bar{p}_s$ , leading to

$$p_m' - p_s' = 0.25 \rho (v_t^2 - \overline{v_t^2}) \quad [5]$$

where  $p_m' = p_m - \bar{p}_m$ , etc. The mean-square error in the measured pressure is just the mean of the square of Equation [5], viz.,

$$\overline{(p_m' - p_s')^2} = 0.5 (\rho \overline{v_t^2})^2 \quad [6]$$

To obtain the above equation, the relations  $\overline{v_t^4} = 3(\overline{v_t^2})^2$  and  $\overline{v_t^2} = 2u^2$  have been used, based on the assumptions that the turbulent velocities are Gaussian and also isotropic.

The error indicated by Equation [6] is somewhat larger than estimates of the magnitude of the static pressure fluctuations in isotropic turbulence; e.g., Batchelor<sup>13</sup> gives  $\overline{p_s'^2} = 0.34 (\rho u^2)^2$ . Accordingly, it does not seem possible to use a probe tube to measure the true static-pressure fluctuations in isotropic turbulence.

---

\*The fact that the correlation coefficient  $\overline{u_p}$  was found to be less than 0.01 (see Section 3.2) also indicates that B is less than 0.01.

However, the fluctuations measured in the situation under discussion, behind a cylinder, were significantly larger than this error. For example, at  $x/D = 24$  the velocity fluctuation is  $\tilde{u}/U_0 = 0.11$ , and this value in Equation [6] gives a mean-square error of  $7.5 \times 10^{-5} (\rho U_0^2)^2$ . On the other hand, the measured mean-square pressure (shown in Figure 8) is  $3.1 \times 10^{-4} (\rho U_0^2)^2$ , which is some four times larger. Accordingly, assuming that the true static pressure is not correlated with the error, then the true mean-square value is  $3/4$  of the measured mean square. Returning to rms values, the corrected value of the measured coefficient of fluctuating static pressure is thus  $\tilde{p}_s / \frac{1}{2} \rho U_0^2 = 0.030$ .

#### 4.2 COMPARISON WITH THEORY

It is of interest to compare this corrected value of the fluctuating static pressure with theoretical estimates. As just mentioned, the calculated value for isotropic turbulence is smaller. Superimposing a uniform mean flow upon the turbulence would not change this value. The flow behind a cylinder is far from uniform, however, since there is a large and variable mean shear across the wake. A crude approximation to the actual flow is the idealized case considered by Kraichnan<sup>14</sup> of isotropic and homogeneous turbulence superimposed upon a uniform mean shear. If the mean shear is large enough, the main contribution to the fluctuating pressure is what Kraichnan calls "turbulence-shear interaction." The coefficient of the fluctuating pressure due to this interaction is given by

$$\tilde{p}_s / \frac{1}{2} \rho U_0^2 = 1.46 (\tilde{u}/U_0) (L/U_0) (\partial U/\partial y) \quad [7]$$

where  $\partial U/\partial y$  is the mean shear and  $L$  is a correlation length, defined so that the longitudinal velocity cross-correlation varies with longitudinal separation  $x'$  as  $e^{-|x'|/L}$ .

This correlation length can be estimated from the measured frequency spectrum of the velocity, since the longitudinal correlation function is the Fourier transform of the longitudinal wave-number spectrum. If the velocity field is assumed to be convected at a local velocity  $U$ , differing from the free-stream velocity  $U_0$ , then the correlation function  $e^{-|x'|/L}$  has a frequency spectrum  $F(S)$  given by

$$F(S) = \frac{4 (U_o/U) (L/D)}{1 + 4n^2 S^2 (U_o/U)^2 (L/D)^2} \quad [8]$$

where  $S$  is the Strouhal number  $nD/U_o$ . The observed spectral shape is indeed very similar to that given by Equation [8]. The length  $L$  can be evaluated from the observed spectrum by equating the zero-frequency value of Equation [8], which is simply its numerator, to the low-frequency asymptote of the measured spectrum.

If Equation [7] is used to estimate the pressure fluctuations behind a cylinder, some sort of space average of the fluctuating velocity and mean shear in the wake is required. Instead of attempting to find the proper average values, the maximum values of these quantities have been inserted into Equation [7] in order to indicate the largest possible value of the turbulence-shear contribution to the fluctuating pressure. The actual values used in the calculation, made for  $x/D = 24$ ,  $y/D = 1/2$ , are:

$$U/U_o = 0.8 \quad \text{from Fage's Figure 14a (Reference 1);}$$

$$(U_o/D)F(0) = 5 \quad \text{from Figure 8 of this report;}$$

$$\partial U/\partial y = 0.15 (U_o/D) \quad \text{from Fage, ibid;}$$

$$L/D = 1 \quad \text{from Equation [8] and Figure 8 of this report.}$$

With these values, the calculated pressure coefficient  $\tilde{p}/\frac{1}{2}\rho U_o^2$  is 0.024. This is somewhat smaller than the corrected measured value of 0.030. To this must be added the contribution of what Kraichnan calls "turbulence-turbulence interaction," with a calculated pressure coefficient of 0.017. If the two contributions were uncorrelated with each other, their resultant would be 0.029. This agreement with the measured value is entirely fortuitous, however, since the calculation is based on maximum values, so that the calculated value should be larger than the measured value. The agreement does indicate, however, that the measured value is reasonable.

#### 4.3 THE SPECTRA

The most striking feature of the measured spectra of pressure and velocity shown in Figure 8 is the similarity of their shapes. The validity

of the measured pressure spectrum is based on the assumption that the perturbation of the true static pressure caused by the probe tube is about the same at all frequencies. This would be the case if the perturbation was associated only with fluctuating velocities, as expressed in the perturbing terms in Equation [3]. At high frequencies, however, acceleration terms might contribute to the error, and these were not taken into account in the previous calculation of the error made for the total wide-band signal. Acceleration terms would tend to raise the high-frequency portion of the measured pressure spectrum.

#### 4.4 COMPARISON WITH OTHER DATA

Kobashi<sup>6</sup> has reported some measurements of fluctuating static pressure behind a cylinder but, unfortunately, there seem to be typographical errors in his published data which make a comparison impossible. The magnitude of the fluctuating pressure shown in his Figure 16 indicates a pressure coefficient  $\tilde{p}_s / \frac{1}{2} \rho U_o^2$  of about 0.3; this seems much too large so far downstream (at  $x/D = 42$ ). The magnitude of the cross-correlation  $\overline{up}_s$  shown in his Figure 17 corresponds to a correlation coefficient  $\overline{up}_s / \tilde{up}_s$  of about  $10^{-4}$ ; if this is indeed the value, it certainly agrees with the present observation that the correlation coefficient is less than 0.01.

#### 4.5 FLUCTUATING TOTAL HEAD

The results indicate that the fluctuating total head can be used as an indication of the magnitude and spectrum of the fluctuating velocity to an accuracy of perhaps 10 percent. However, the lack of complete correlation between the signal from the total-head probe and the signal from an adjacent hot wire indicates that the total head contains a component which is not correlated with the fluctuating velocity.

The source of this uncorrelated component is not known. It cannot be the fluctuating static pressure because this is too small; the measured pressure coefficient of the static pressure is only 0.035, whereas the coefficient of the total-head pressure is 0.22. The existence of this uncorrelated component indicates that caution must be observed when using

total-head probes to denote velocity fluctuations.\*

---

\*At the AGARD meeting in Brussels it was suggested that the low value of the measured correlation may be caused by phase shift in the probe tube. Although the phase shift was never measured, it is believed to be too small to account for the discrepancy.

An estimate of the reduction in cross correlation resulting from a phase shift of the total-head signal can be obtained by assuming that the total-head signal has two components, one completely correlated with the wire signal and the other independent of and uncorrelated with the wire signal. If the total-head signal were shifted in phase a constant angle  $\theta$  at all frequencies, then the cross correlation of the correlated components would be reduced by the factor  $\cos \theta$ , whereas the independent components would remain uncorrelated, so the correlation coefficient of the two signals would be reduced simply by the factor  $\cos \theta$ .

The phase shift in the probe tube undoubtedly increases with frequency, but to obtain an upper-bound estimate, assume that the shift has a constant value equal to its value at a "cut-off" frequency where the spectral density has fallen to 1/10 of its low-frequency value. Using this value will certainly give an extreme estimate of the effect, since higher frequencies do not contribute much to either the total signal or the correlations. From the spectra of Figure 7, this "cut-off" corresponds to a Strouhal number of about 0.5, thus corresponding to a real frequency of about 150 cycles/sec at a speed of 28 ft/sec. As shown in Figure 3, this frequency is about 1/6 the frequency at which the probe sensitivity falls to half its low-frequency value. If the probe tube is critically damped, the response curve shown in Figure 3 of Reference 9 can be used to show that the phase shift at frequencies up to 150 cycles/sec is not more than 20 deg. This shift would reduce the correlation coefficient by a factor of only about 0.94, but the difference between the two correlations shown in Figure 11 is much larger.

## 5. CONCLUSIONS

These measurements of the fluctuating static and total-head pressures in the turbulent wake behind a cylinder lead to the following conclusions:

1. A static-pressure probe tube will indicate a fluctuating pressure whose mean-square value is higher than the true value by an amount about  $0.5(\overline{\rho u^2})^2$ . This error is of the same order as the magnitude of the pressure fluctuations in isotropic turbulence. However, the pressure fluctuations measured in the wake behind a cylinder are significantly larger than the error, indicating that probe tubes can be used to measure static-pressure fluctuations in flows with large mean shear.

2. The spectrum of the fluctuating static pressure behind a cylinder has the same shape as the spectrum of the longitudinal velocity at the same location.

3. The instantaneous fluctuating total head can be used to indicate the magnitude of longitudinal velocity fluctuations. For unknown reasons, however, the fluctuating total head is not completely correlated with the fluctuating longitudinal velocity.

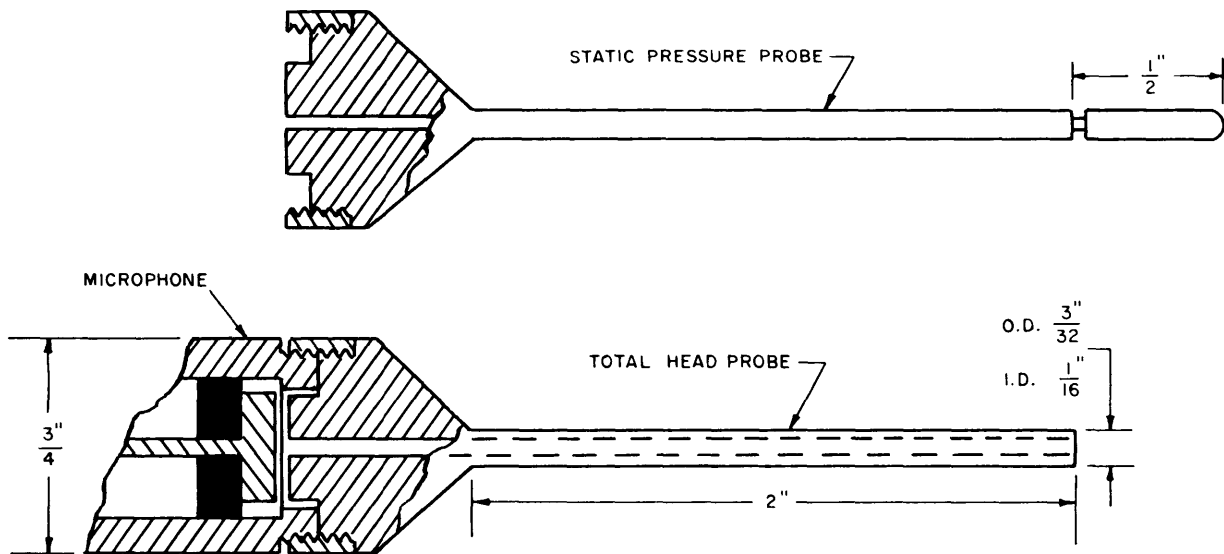


Figure 1 – Schematic of the Total-Head Probe Attached to the Capacitance Microphone Cartridge, and the Static-Pressure Probe

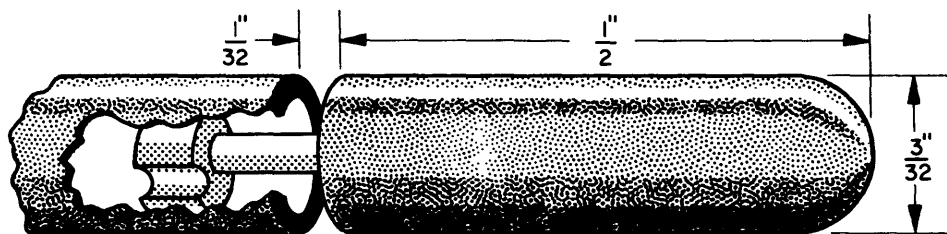


Figure 2 – Annular Ring Slit in the Static-Pressure Tube

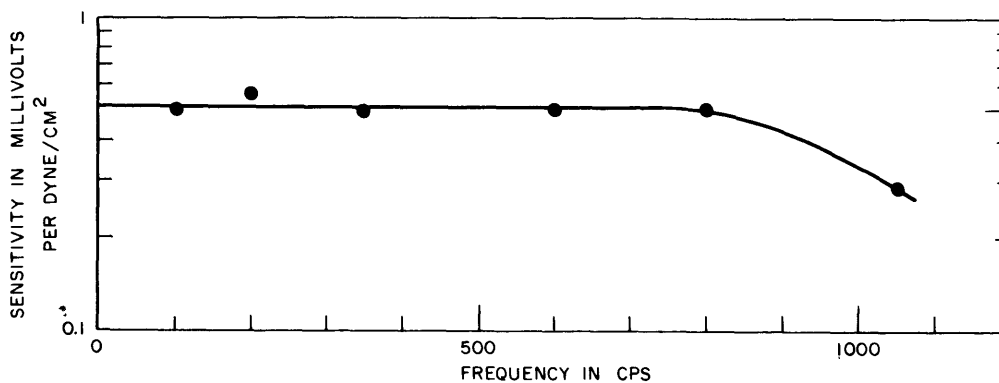


Figure 3 – Response of Total-Head Probe Tube and Microphone



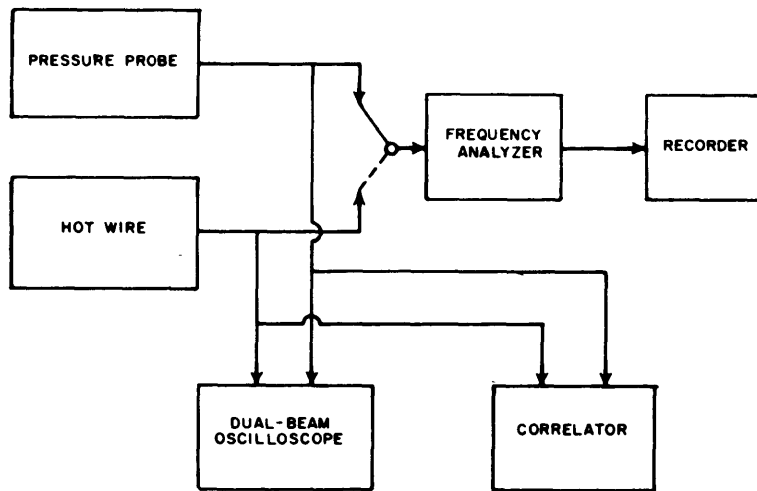


Figure 4 – Block Diagram of Electronic Instrumentation

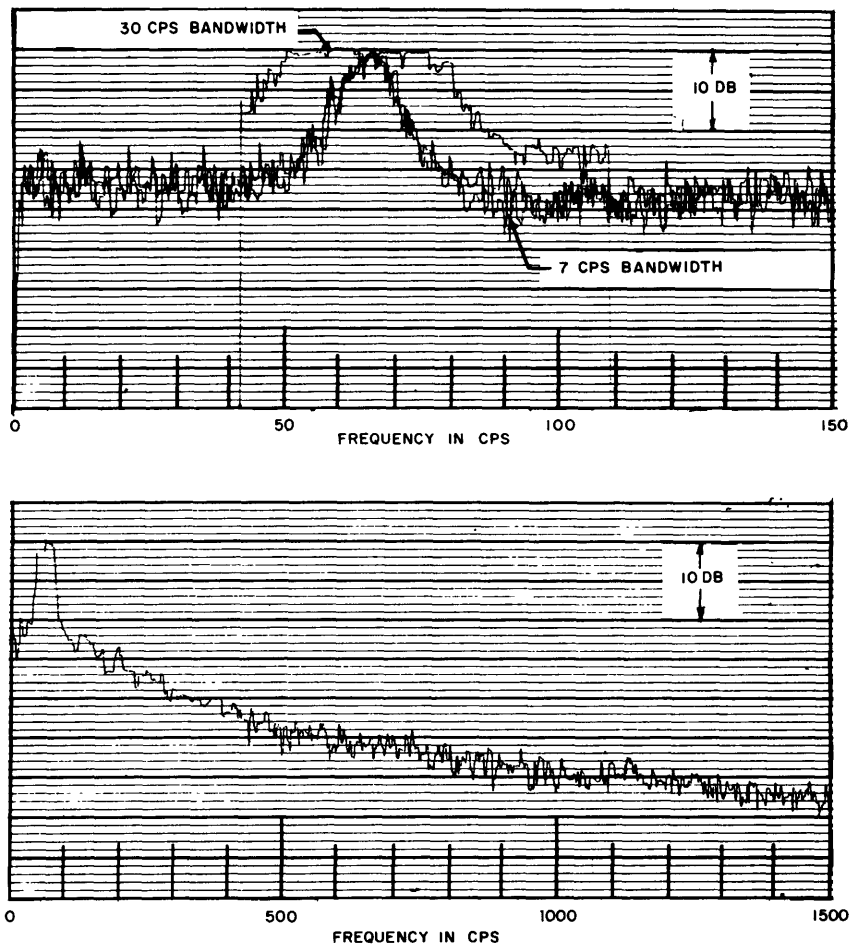


Figure 5 – Typical Spectra, Plotted by Automatic Recording Frequency Analyzer, for Two Frequency Ranges

The upper chart has superimposed plots for two bandwidths.  
 The ordinate is a logarithmic scale, with each division corresponding to 1 db.

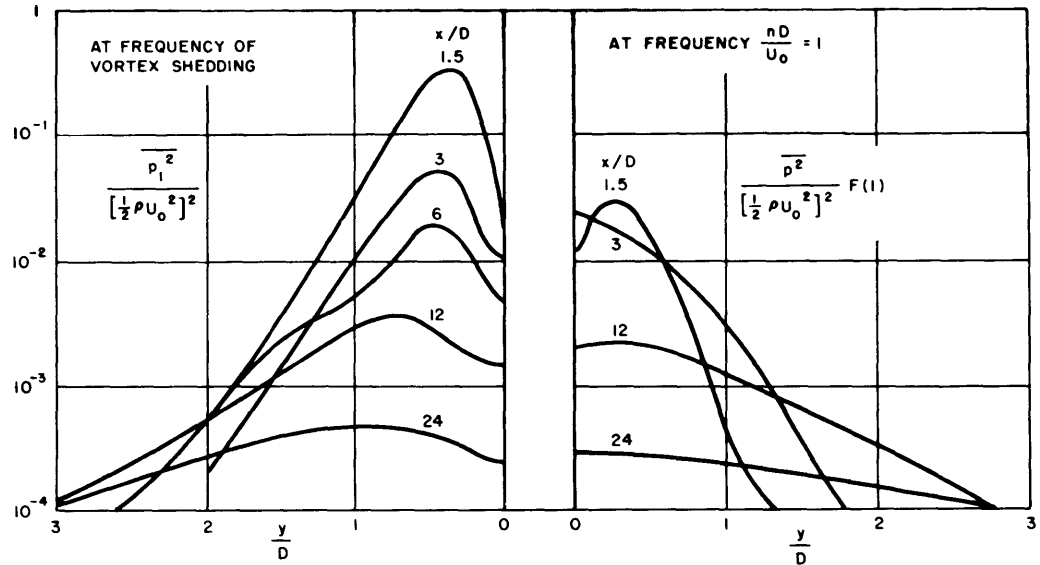


Figure 6 – Fluctuating Static Pressure, as a Function of Transverse Coordinate  $y$ , at Various Downstream Locations

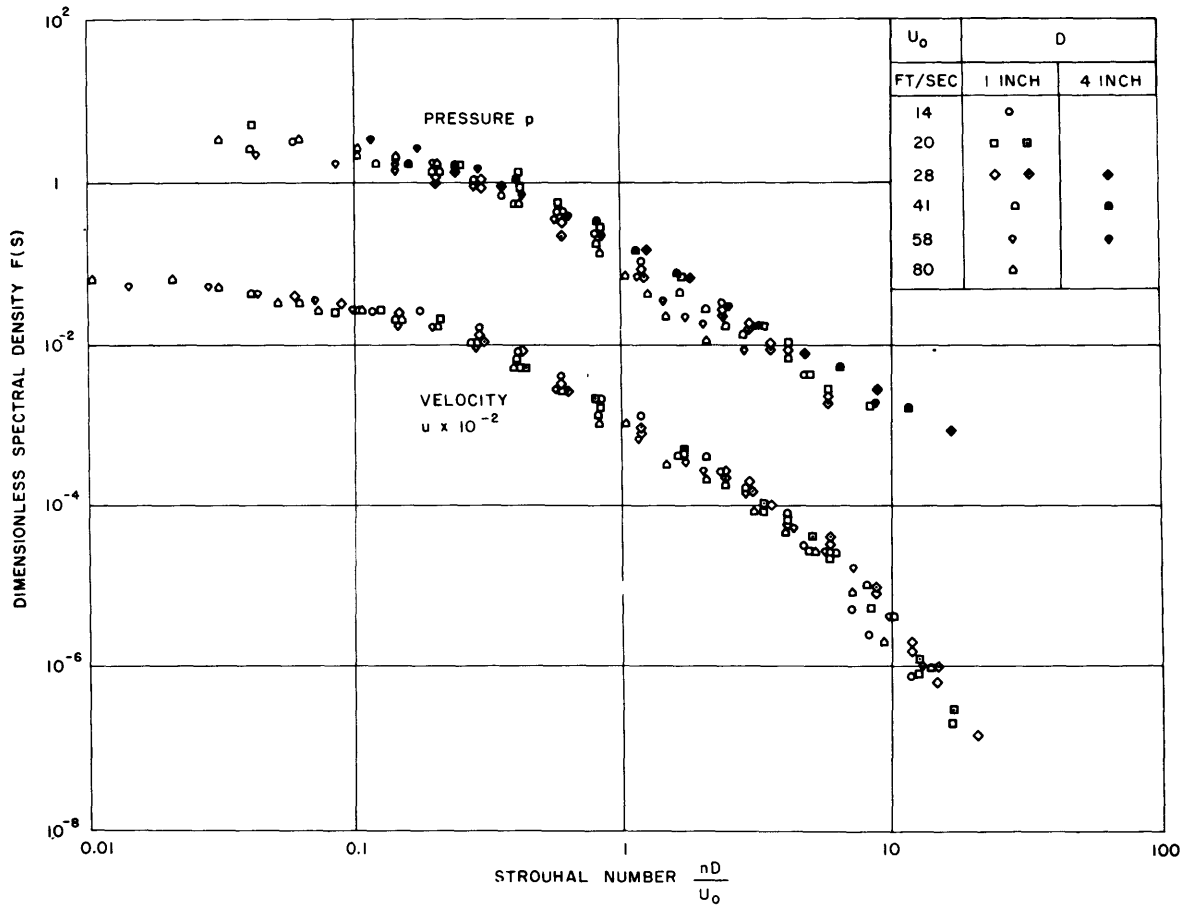


Figure 7 – Nondimensional and Normalized Spectral Density of Fluctuating Static Pressure and Velocity at  $x/D = 24$ ,  $y/D = 1/2$

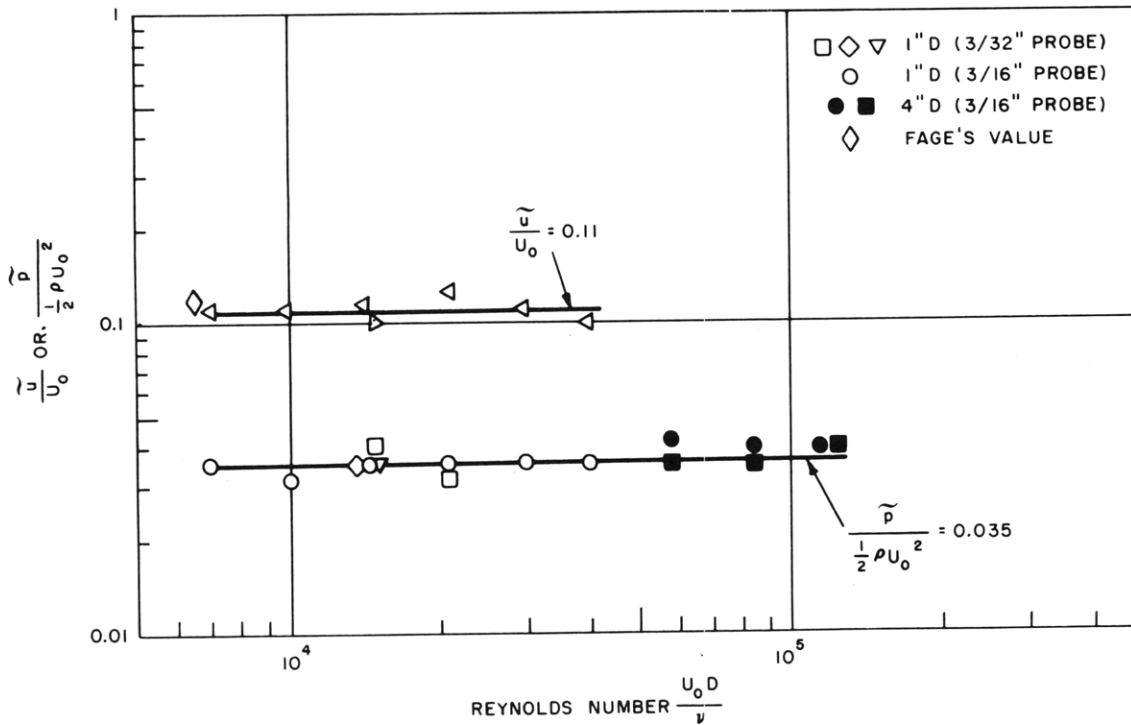
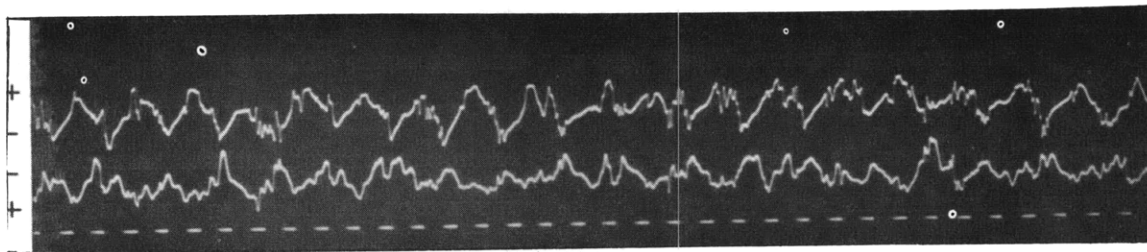
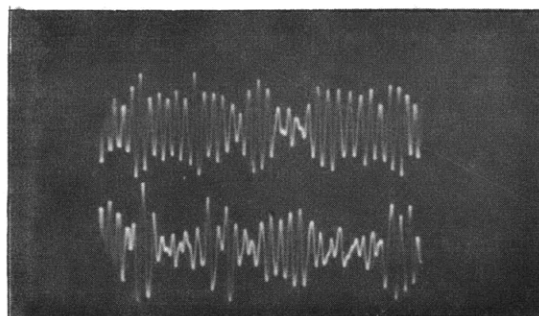


Figure 8 - Measured Root-Mean-Square Value of Total Fluctuating Static Pressure and Velocity, as a Function of Reynolds Number, at  $x/D = 24$ ,  $y/D = 1/2$

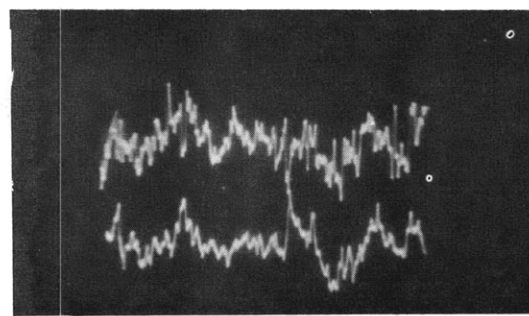


Motion picture strip at  $x/D = 3$



$x/D = 3$

60-80 cy/sec filter



$x/D = 24$

Figure 9 - Simultaneous Oscillograms of Fluctuating Velocity and Static Pressure

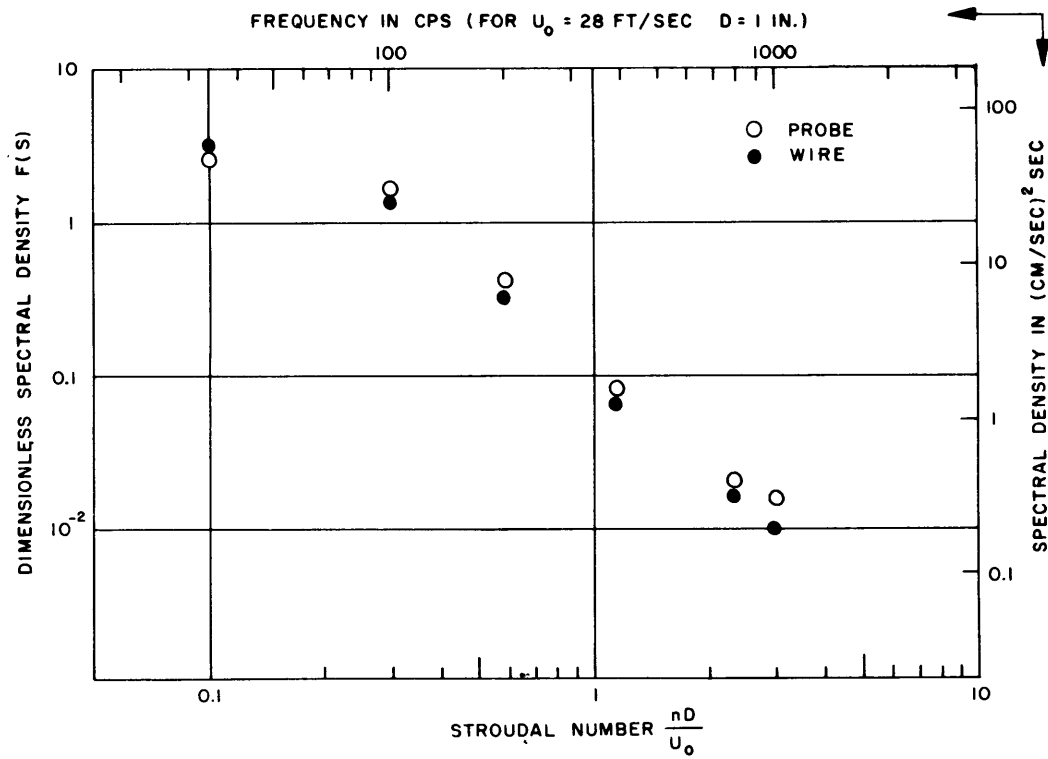


Figure 10 – Comparison of the Spectral Densities Determined with a Total-Head Probe and a Hot Wire

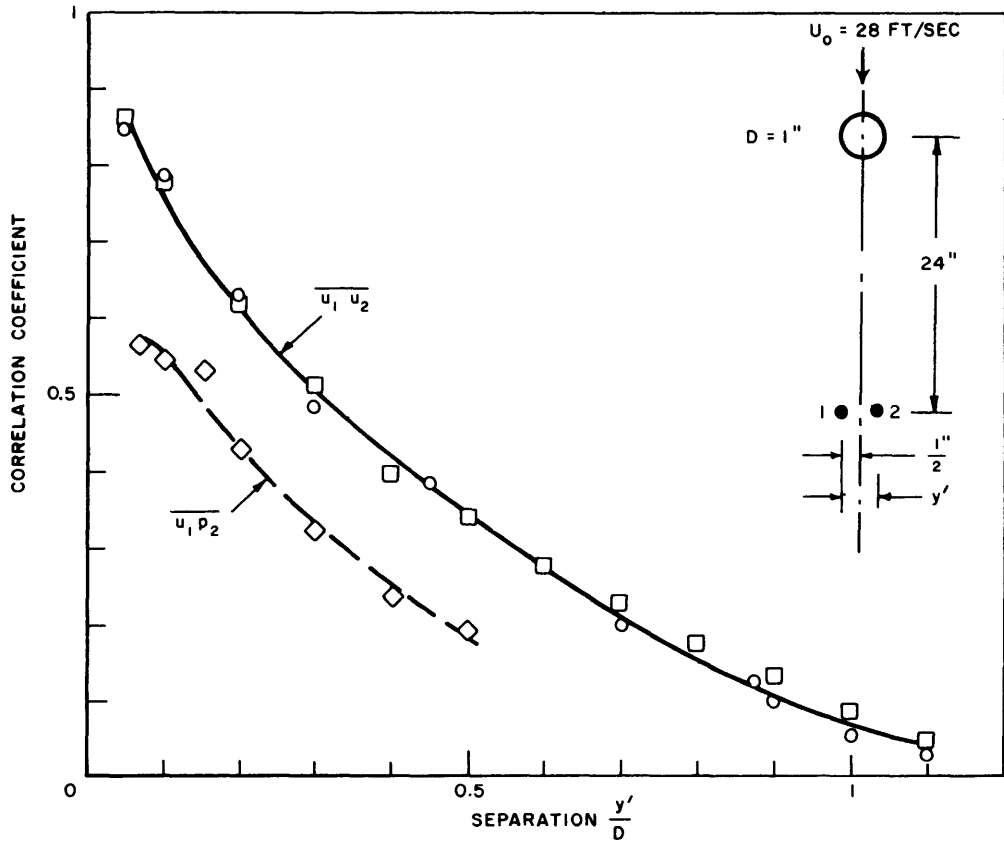


Figure 11 – Transverse Correlation ( $\overline{u_1 p_2}$ ) of Signals from a Total-Head Probe and a Hot Wire Compared with Correlation ( $\overline{u_1 u_2}$ ) of Signals from Two Wires

## 6. REFERENCES

1. Fage, A., "On the Static Pressure in Fully-Developed Turbulent Flow," Proc. Royal Society, A, Vol. CLV (1936), p.576.
2. Strasberg M., and Cooper, R. D., "Measurements of the Fluctuating Pressure and Velocity in the Wake of a Cylinder," Proc. 9th International Congress of Applied Mechanics, Vol. 2, (1957), p.384.
3. Ippen, A. T., Tankin, R. S., and Raichlen, F., "Turbulent Measurements in Free Surface Flow with an Impact Tube," Massachusetts Institute of Technology, Hydrodynamics Laboratory (Dept Civil and Sanitation Engineering) Technical Report 20 (Jul 1955).
4. Bruer L. J. F., and de Haan, R. E., "Total-Head Measurements in Fluctuating Flows," Journal Applied Mathematics and Physics (ZAMP), Vol. IXb (1958), p.162.
5. Rouse, H., "Cavitation in the Mixing Zone of a Submerged Jet," La Houille Blanche, Vol. 8 (1953), p.9.
6. Kobashi, Y., "Measurements of Pressure Fluctuation in the Wake of a Cylinder," Journal Physical Society of Japan, Vol. 12 (1957), p.533; also Journal of Aerospace Sciences, Vol. 27, (1960), p.149.
7. Perkins F. E., and Eagleson, P. S., "Development of a Total-Head Tube for High-Frequency Pressure Fluctuations in Water," Massachusetts Institute of Technology, Hydrodynamics Laboratory (Dept Civil and Sanitation Eng.) Technical Note 5 (Jul 1959).
8. Taback, I., "The Response of Pressure Measuring Systems to Oscillating Pressures," National Advisory Committee of Aeronautics TN 1819, (Feb 1949).
9. Iberall, A. S., "Attenuation of Oscillatory Pressures in Instrument Lines," Journal of Research, National Bureau of Standards, Vol. 45 (1950) p.85.
10. Beranek, L. L., "Acoustical Measurements," John Wiley and Sons (1949); see p.123 et seq.

11. Roshko, A., "On the Development of Turbulent Wakes from Vortex Streets," National Advisory Committee for Aeronautics Report 1191 (1954).

12. Goldstein, S., "A Note on the Measurement of Total Head and Static Pressure," Proc. Royal Society A, Vol. CLV (1936), p.570.

13. Batchelor, G. K., "Pressure Fluctuations in Isotropic Turbulence," Proc. Cambridge Philosophical Society, Vol. 47 (1951), p.359.

14. Kraichnan, R., "Pressure Field within Homogeneous Anisotropic Turbulence," Journal Acoustical Society of America, Vol. 28 (1956), p.64.

15. Corcos, G. M., "Pressure Measurements in Unsteady Flows," Univ. California Institute of Engineering Research, Report Series No. 183, Issue No. 1 (Jan 1962).

**BLANK**



INITIAL DISTRIBUTION

Copies		
5	CHBUSHIPS	1 ONR (Code 438)
	3 Tech Lib (Code 210L)	
	1 Lab Mgt (Code 320)	1 Bureau of Standards
	1 Ship Sil Br. (Code 345)	Attn: P. Klebanoff
1	DIR ORL, Penn State	
1	CDR, USNOTS China Lake	
1	CO & DIR, USNEL	
1	CO & DIR USNUSL	
1	Lewis Res Ctr, NASA	
	Attn: Dr. J. S. Serafini	
1	Langley Res Ctr, NASA	
	Attn: H. H. Hubbard	
20	DDC	
1	U. of Calif., Berkeley	
	Attn: Prof. G. M. Corcos	
1	Jet Propulsion Lab	
	Attn: Dr. J. Laufer	
1	Bolt, Beranek and Newman, Inc.	
1	Hydronautics, INC	
1	DL, SIT	
1	MIT, Attn: Prof. A. T. Ippen	
1	MIT, Attn: Prof. E. L. Mollo-Christensen	
1	MIT, Attn: Prof. M. A. Kolpin	
1	Johns Hopkins Univ	
	Attn: Prof. L. S. Kovasnay	
1	Johns Hopkins Univ	
	Attn: Prof. S. Corrsin	
1	Yale University	
	Attn: Dr. A. L. Kistler	
1	Univ. Michigan	
	Attn: Prof. W. W. Willmarth	
2	Univ. of California (LA)	
	Attn: Dr. A. Powell (Dept of Eng)	
	Attn: Prof. I. Rudnick (Physics Dept)	



MIT LIBRARIES

DUPL



3 9080 02754 4706

